

## Observation of $e^+e^- \rightarrow \chi_{c1}$ at BESIII

---

**Stefano Spataro\*** on behalf of the BESIII collaboration

*University of Turin and INFN,  
via Pietro Giuria 1, I-10125, Turin, Italy*

*E-mail:* [spataro@to.infn.it](mailto:spataro@to.infn.it)

In electron-positron annihilation, the process  $e^+e^- \rightarrow \chi_{c1}$  can occur via the production of two virtual photons or through neutral current, therefore being suppressed with respect to the normal annihilation process via one virtual photon. Using a dedicated scan sample around the  $\chi_{c1}$  mass, the direct production of  $\chi_{c1}$  has been established for the first time. This provides a new approach for the study of the internal nature of hadrons. We report also the search for the direct production of the  $X(3872)$  state, where no significant signal has been observed and we estimated an improved upper limit.

*42nd International Conference on High Energy Physics (ICHEP2024)  
18-24 July 2024  
Prague, Czech Republic*

---

\*Speaker

## 1. Introduction

In  $e^+e^-$  collisions, the dominant mechanism for the direct production of hadronic resonances is the transition through a virtual photon; indeed, only vector states ( $J^{PC} = 1^{--}$ ) has been observed so far. Nevertheless, it is predicted that also  $C$ -even states are produced, through annihilation of two time-like virtual photons or via neutral currents. These processes have been searched for in the past, without any significant signal.

In the charmonium region, a good candidate for the search of direct production of  $J^{PC} = 1^{++}$  states is the  $\chi_{c1}$  meson. The production rate is proportional to its electronic width, and several predictions are available since 1970s [1]. According to the unitarity limit, the lower limit of the electronic width has been estimated to be  $\Gamma_{ee} > 0.044$  eV; the Vector Dominance Model suggests a width of  $\Gamma_{ee} = 0.46$  eV. Revisited predictions using the Vector Dominance Model [2] or calculations in non-relativistic QCD [3] estimate the electronic width to be in the order of 0.1 eV.

More recently, the authors of Ref. [4] studied the direct production of  $\chi_{c1}$  and  $\chi_{c2}$  states in  $e^+e^-$  collisions following the strategy of Refs. [1], by including the interference between the dominant decay  $\chi_{cJ} \rightarrow \gamma J/\psi \rightarrow \gamma \mu^+ \mu^-$  and the background processes  $e^+e^- \rightarrow \gamma \mu^+ \mu^-$ . They predicted a width of  $\Gamma_{ee} = 0.43$  eV, and that the interference produces a distortion of the line shape of the  $\chi_{c1}$  meson. According to the predictions, an increase of the cross section above the background should appear below the  $\chi_{c1}$  mass value, while a dip just after the mass peak; at the  $\chi_{c1}$  peak position the cross section is expected to be compatible to the expectation from the continuum process.

We report the first observation by BESIII of the  $e^+e^- \rightarrow \chi_{c1}$  direct production, as well the measurement of the  $\Gamma_{ee}$  electronic widths. Moreover, we report the measurement of the  $e^+e^- \rightarrow J/\psi \pi^+ \pi^-$  cross section around the  $X(3872)$  mass, where no signal evidence of the  $X(3872)$  direct production has been found and the upper limit has been estimated.

## 2. Description of BEPCII and the BESIII detector

The BESIII detector [5] records symmetric  $e^+e^-$  collisions provided by the BEPCII storage ring [6] in the center-of-mass energy range from 1.84 to 4.95 GeV, with a peak luminosity of  $1.1 \times 10^{33} \text{ cm}^{-2}\text{s}^{-1}$  achieved at  $\sqrt{s} = 3.773$  GeV. BESIII has collected large data samples in this energy region [7]. The cylindrical core of the BESIII detector covers 93% of the full solid angle and consists of a helium-based multilayer drift chamber (MDC), a time-of-flight system (TOF), and a CsI(Tl) electromagnetic calorimeter (EMC), which are all enclosed in a superconducting solenoidal magnet providing a 1.0 T magnetic field. The solenoid is supported by an octagonal flux-return yoke with resistive plate counter muon identification modules interleaved with steel. The charged-particle momentum resolution at 1 GeV/ $c$  is 0.5%, and the  $dE/dx$  resolution is 6% for electrons from Bhabha scattering. The EMC measures photon energies with a resolution of 2.5% (5%) at 1 GeV in the barrel (end cap) region. The time resolution in the plastic scintillator TOF barrel region is 68 ps, while that in the end cap region was 110 ps. The end cap TOF system was upgraded in 2015 using multigap resistive plate chamber technology, providing a time resolution of 60 ps.

### 3. Observation of $e^+e^- \rightarrow \chi_{c1}$

In 2017, BESIII has performed a dedicated  $\chi_{c1}$  mass scan, where data were collected at four different center-of-mass energies (3.5080 GeV, 3.5097 GeV, 3.5104 GeV, and 3.5146 GeV), corresponding to a total integrated luminosity of 457.8 pb<sup>-1</sup>: the first two scan points below the  $\chi_{c1}$  mass, where a constructive interference effect between the signal process and the irreducible background processes is expected; the third point slightly below the  $\chi_{c1}$  mass, so that a minimal effect is expected; the fourth scan point above the  $\chi_{c1}$  mass, where we expect a reduction of events with respect to the non reducible background. In case of no interference, a peak over the background is expected at the  $\chi_{c1}$  mass.

To verify the background description, we have also analysed four control samples with a total integrated luminosity of 6294 pb<sup>-1</sup>, ( $\sqrt{s} = 3.581$  GeV, 3.670 GeV,  $\sqrt{s} = 3.773$  GeV and 4.178 GeV).

The  $\chi_{c1}$  is reconstructed via its radiative decay  $\chi_{c1} \rightarrow \gamma J/\psi$ , with the subsequent decay  $J/\psi \rightarrow \mu^+\mu^-$ . The  $J/\psi \rightarrow e^+e^-$  mode is not used since the background level from Bhabha process ( $e^+e^- \rightarrow e^+e^-$ ) is two orders of magnitude higher than  $e^+e^- \rightarrow \mu^+\mu^-$ .

In the MonteCarlo simulation, we use the PHOKHARA [9] event generator to describe the signal process ( $e^+e^- \rightarrow \chi_{c1} \rightarrow \gamma J/\psi \rightarrow \gamma\mu^+\mu^-$ ), the irreducible background processes ( $e^+e^- \rightarrow \gamma_{\text{ISR}} J/\psi \rightarrow \gamma_{\text{ISR}} \mu^+\mu^-$  and  $e^+e^- \rightarrow \gamma_{\text{ISR}} \mu^+\mu^-$ ), and the interference between them. Angular distributions for the signal process are implemented into the PHOKHARA generator using Ref. [4], while the background ISR processes are modeled using Ref. [9].

A full reconstruction method is used to select  $\gamma\mu^+\mu^-$  candidate events. The charged tracks and photons are selected as described in Ref. [10], and muon tracks are identified by their energy deposit in the Electromagnetic Calorimeter. A four constraint kinematic fit is applied on the two charged tracks and the photon constraining the total reconstructed four momentum to that of the initial state. If more photons are reconstructed in the event, the combination with the minimum  $\chi^2_{4C}$  is selected. We suppress background events from ISR processes requiring the polar angle of the best photon candidate to be  $|\cos \theta_\gamma| < 0.80$ .

To validate our Monte Carlo description, we simulate the irreducible background processes using the PHOKHARA event generator and test its prediction by using control samples from data, in which the signal process is absent. We perform a two-dimensional fit to the  $\mu^+\mu^-$  invariant mass ( $M_{\mu^+\mu^-}$ ) distribution and the  $|\cos \theta_\mu|$  distribution with non-interfering signal and background components, and since we found discrepancies, we carry out a two-dimensional correction to the distributions of  $M_{\mu^+\mu^-}$  and  $|\cos \theta_\mu|$  by re-weighting MC simulated events to correct for the uncertainty in  $\Gamma_{ee}^{J/\psi}$  and the limitations of the PHOKHARA MC generator. After applying these correction factors, the signal is consistent with zero within one standard deviation for all control samples.

After applying the corrections to the Monte Carlo samples, discrepancies between data and Monte Carlo prediction around the  $J/\psi$  peak are studied for the four data points close to the  $\chi_{c1}$  mass.

In order to extract the number of signal events, the  $M_{\mu^+\mu^-}$  and  $|\cos \theta_\mu|$  distributions are fitted at each data sample individually using a two-dimensional unbinned maximum likelihood fit method. The line-shapes for the contributions from the  $\chi_{c1}$  signal, the irreducible background and the

interference term are derived from the corresponding individual MC simulations after corrections. The numbers of  $\chi_{c1}$  ( $N_{\chi_{c1}}$ ) and background events ( $N_{bg}$ ) are free parameters, while the interference term ( $N_{int}$ ) is written as  $f \cdot \sqrt{N_{\chi_{c1}} \cdot N_{bg}}$ , where the factor  $f$  is determined from signal MC. Since the numbers depend on the values of the electronic width  $\Gamma_{ee}$  for the  $\chi_{c1}$  and the phase  $\phi$  between the amplitudes, which are model-dependent, we produced several MC data samples scanning different values for the  $\chi_{c1}$  and  $\phi$  parameters, and extracted the optimal values selecting the combination with the best likelihood of the combined fit. The  $-\ln L$  distribution as a function of  $\Gamma_{ee}$  and  $\phi$  is shown in Fig. 1. The best  $\Gamma_{ee}$  and  $\phi$  parameters are determined to be  $(0.12^{+0.08}_{-0.07})$  eV and  $(205.0^{+10.0}_{-17.0})^\circ$ , respectively, where the uncertainty corresponding to 68.3% C.L. is statistical only.

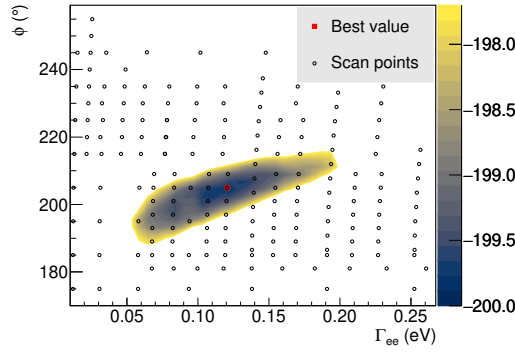


**Figure 1:** The 68.3% C.L. contour of  $\Gamma_{ee}$  and  $\phi$  on a distribution of log-likelihood ( $-\ln L$ ) values. The black open circles are the parameter points with which MC samples are produced. The red point (0.12 eV, 205.0°) represents the point where the likelihood value is maximum.

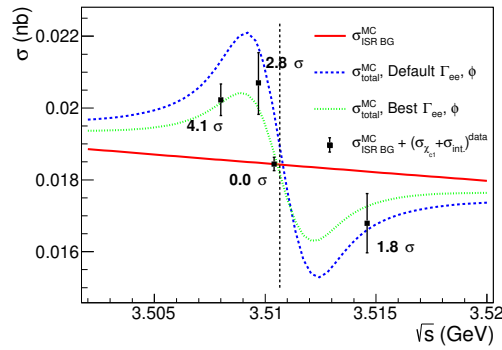


**Figure 2:** Energy dependence of the cross section of the process  $e^+e^- \rightarrow \gamma J/\psi \rightarrow \gamma \mu^+ \mu^-$  including (blue and green dashed lines) and not including (red solid line) the direct production of the  $\chi_{c1}$ .

Using the optimal values obtained in this way, significant signal components are seen at  $\sqrt{s} = 3.5080$  GeV and 3.5097 GeV with  $N_{sig} = N_{\chi_{c1}} + N_{int}$  (and its statistical significance) determined to be  $210 \pm 52$  ( $4.1\sigma$ ) and  $63 \pm 24$  ( $2.8\sigma$ ), respectively. The signal component is not significant at  $\sqrt{s} = 3.5104$  GeV with  $N_{sig} = 0^{+16}_{-19}$  ( $0.0\sigma$ ). A negative signal component is seen at

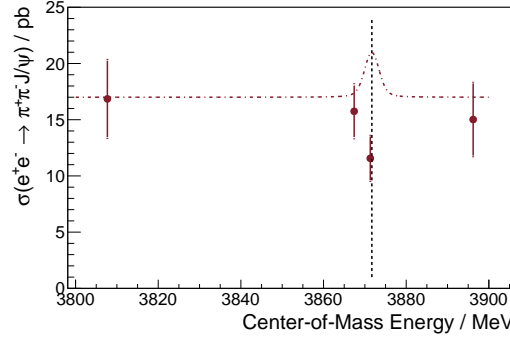


**Figure 3:** Cross section of  $e^+e^- \rightarrow \pi^+\pi^- J/\psi$ . The results of both  $J/\psi$  decay modes are combined. The error bars represent the total uncertainties, *i.e.*, the quadratic sum of the statistical and systematic uncertainties. The dashed vertical line indicates the peak position of  $X(3872)$ . The dot-dashed curve shows an illustration of expected line-shape assuming  $\Gamma_{ee} \times \mathcal{B}(X(3872) \rightarrow \pi^+\pi^- J/\psi) = 0.013$  eV.

$\sqrt{s} = 3.5146$  GeV with  $N_{\text{sig}} = -40 \pm 22$  ( $1.8\sigma$ ). The combined statistical significance, obtained by adding the log-likelihoods ( $-\ln L$ ) from each of the four data samples, is  $5.3\sigma$ .

The cross section of the signal component and its uncertainty is calculated as  $\sigma_{\text{sig}} \equiv (\sigma_{\chi_{c1}} + \sigma_{\text{int.}})^{\text{data}} = N_{\text{sig}}/(\mathcal{L} \cdot \epsilon)$ , where the efficiency  $\epsilon$  is calculated from the simulated signal MC samples. The sum of  $\sigma_{\text{sig}}$  and  $\sigma_{\text{ISR BG}}$  at each  $\chi_{c1}$  scan point is shown in Fig. 2 (black dots), which is in good agreement with the theoretical prediction [4]. Here  $\sigma_{\text{ISR BG}}$  is fixed using the PHOKHARA generator.

This analysis is published in Ref. [11].

#### 4. Search for $e^+e^- \rightarrow X(3872)$

The  $X(3872)$  state, also called  $\chi_{c1}(3872)$ , is probably the best known representative of the exotics states, which do not fit into the conventional charmonium spectrum [12]. The  $J^{PC}$  of the  $X(3872)$  state is measured to be  $1^{++}$  [13], which allows suppressed formation in  $e^+e^-$  collisions via two-photon fusion as seen for the  $\chi_{c1}$ . The current upper limit is  $\Gamma_{ee} \times \mathcal{B}(X(3872) \rightarrow \pi^+\pi^- J/\psi) < 0.13$  eV at 90% confidence level (C.L.), determined by BESIII via the initial-state radiation (ISR) process [14]. We searched for the direct production of  $X(3872)$  by measuring the cross section  $\sigma(e^+e^- \rightarrow \pi^+\pi^- J/\psi)$  around the  $X(3872)$  mass, using four data sets collected by the BESIII detector where two were recorded in the vicinity of the  $X(3872)$  mass, one directly on the  $X(3872)$  peak with c.m. energy of 3871.3 MeV (on-resonance), and the other one about 4 MeV below the peak at 3867.4 MeV (off-resonance). In this case there is no interference between the resonant and continuum parts due to their different quantum numbers.

In the process of  $e^+e^- \rightarrow \pi^+\pi^- J/\psi$ , the  $J/\psi$  is reconstructed via lepton pairs  $\ell^+\ell^-$  ( $\ell = e, \mu$ ). The final state  $\pi^+\pi^-\ell^+\ell^-$  consists of four charged tracks with zero net charge. In Fig. 3, the obtained cross-section values are plotted, where the dashed vertical line indicates the location of the  $X(3872)$  peak. The dot-dashed curve is just for illustration and it shows the line-shape assuming a total width of 1.19 MeV and  $\Gamma_{ee} \times \mathcal{B}(X(3872) \rightarrow \pi^+\pi^- J/\psi) = 0.013$  eV, which is arbitrarily chosen as one order of magnitude lower than the previous upper limit [14]. No enhancement of the cross section is observed at the  $X(3872)$  peak; the cross section on-resonance is smaller than that of the off-

resonance region, but given the low statistics this dip is consistent with a flat distribution within  $1\sigma$ . Since the direct production of the  $X(3872)$  is not observed, an upper limit on  $\Gamma_{ee} \times \mathcal{B}$  is determined. For an assumed total width of  $1.19 \pm 0.21$  MeV, the upper limit on  $\Gamma_{ee} \times \mathcal{B}$  is  $7.5 \times 10^{-3}$  eV at 90 % C.L., with an improvement of a factor of about 17 compared to the previous limit [14].

This analysis is published in Ref. [15].

## 5. Summary

BESIII has observed for the first time the direct production of a  $J^{PC} = 1^{++}$  state in electron-positron collisions, in the process  $e^+e^- \rightarrow \chi_{c1}$ . This opens to new searches of this kind, which were tried in the past but without significant results up to date. We searched also for the direct production of  $X(3872)$ , but no significant signal has been observed.

In the coming years, after the upgrade of the BEPC-II accelerator and of the BESIII detector, much higher luminosity will be recorded and more advanced studies will be possible to be carried on.

## References

- [1] J. H. Kühn, J. Kaplan, and E. G. O. Safiani, Nucl. Phys. B **157**, 125 (1979); J. Kaplan and J. H. Kühn, Phys. Lett. B **78**, 252 (1978).
- [2] A. Denig, F. K. Guo, C. Hanhart, and A. V. Nefediev, Phys. Lett. B **736**, 221 (2014).
- [3] N. Kivel and M. Vanderhaeghen, J. High Energ. Phys. **2016**, 32 (2016).
- [4] H. Czyż, J. H. Kühn and S. Tracz, Phys. Rev. D **94**, 034033 (2016).
- [5] M. Ablikim *et al.* [BESIII Collaboration], Nucl. Instrum. Meth. A **614**, 345 (2010).
- [6] C. H. Yu *et al.*, Proceedings of IPAC2016, Busan, Korea, 2016, doi:10.18429/JACoW-IPAC2016-TUYA01.
- [7] M. Ablikim *et al.* [BESIII Collaboration], Chin. Phys. C **44**, 040001 (2020).
- [8] X. Li *et al.*, Radiat. Detect. Technol. Methods **1**, 13 (2017); Y. X. Guo *et al.*, Radiat. Detect. Technol. Methods **1**, 15 (2017); P. Cao *et al.*, Nucl. Instrum. Meth. A **953**, 163053 (2020).
- [9] M. Ablikim *et al.* [BESIII Collaboration], Phys. Rev. D **81**, 094014 (2010).
- [10] M. Ablikim *et al.* (BESIII Collaboration), Phys. Rev. D **104**, 092001 (2021).
- [11] H. Czyż, A. Grzelińska, and J. H. Kühn, Phys. Rev. Lett. **129**, 122001 (2022).
- [12] G. Mezzadri, and S. Spataro, Rev. in. Phys. **8**, 100070 (2022).
- [13] R. Aaij *et al.* LHCb Collaboration, Phys. Rev. Lett. **110**, 222001 (2013).
- [14] M. Ablikim *et al.* [BESIII Collaboration], Phys. Lett. B **749**, 414-420 (2015).
- [15] M. Ablikim *et al.* [BESIII Collaboration], Phys. Rev. D **103**, 032007 (2023).